The Journal of Neuroscience, January 1, 2001, 21(1):169–175

Bcl-X_L–Caspase-9 Interactions in the Developing Nervous System: Evidence for Multiple Death Pathways

Aliya U. Zaidi,[1] Cleta D'Sa-Eipper,[1] Jennifer Brenner,[1] Keisuke Kuida,[2] Timothy S. Zheng,[3] Richard A. Flavell,[4] Pasko Rakic,[5] and Kevin A. Roth[1]

[1]Department of Pathology and Immunology, Division of Neuropathology, Washington University School of Medicine, St. Louis, Missouri 63110, [2]Vertex Pharmaceuticals, Cambridge, Massachusetts 02139-4242, [3]Department of Inflammation, Immunology, and Cell Biology, Biogen, Cambridge, Massachusetts 02142, and Departments of [4]Immunology, and [5]Neurobiology, Yale University School of Medicine New Haven, Connecticut 06520-8011

Programmed cell death is critical for normal nervous system development and is regulated by Bcl-2 and Caspase family members. Targeted disruption of *bcl-x_L*, an antiapoptotic *bcl-2* gene family member, causes massive death of immature neurons in the developing nervous system whereas disruption of *caspase-9*, a proapoptotic *caspase* gene family member, leads to decreased neuronal apoptosis and neurodevelopmental abnormalities. To determine whether Bcl-X_L and Caspase-9 interact in an obligate pathway of neuronal apoptosis, *bcl-x/caspase-9* double homozygous mutants were generated. The increased apoptosis of immature neurons observed in Bcl-X_L-deficient embryos was completely prevented by concomitant Caspase-9 deficiency. In contrast, *bcl-$x^{-/-}$/caspase-9$^{-/-}$* embryonic mice exhibited an expanded ventricular zone and neuronal malformations identical to that observed in mice lacking only Caspase-9. These results indicate both epistatic and independent actions of Bcl-X_L and Caspase-9 in neuronal programmed cell death.

To examine Bcl-2 and Caspase family-dependent apoptotic pathways in telencephalic neurons, we compared the effects of cytosine arabinoside (AraC), a known neuronal apoptosis inducer, on wild-type, Bcl-X_L-, Bax-, Caspase-9-, Caspase-3-, and p53-deficient telencephalic neurons *in vitro*. AraC caused extensive apoptosis of wild-type and Bcl-X_L-deficient neurons. p53- and Bax-deficient neurons showed marked protection from AraC-induced death, whereas Caspase-9- and Caspase-3-deficient neurons showed minimal or no protection, respectively. These findings contrast with our previous investigation of AraC-induced apoptosis of telencephalic neural precursor cells in which death was completely blocked by p53 or Caspase-9 deficiency but not Bax deficiency. In total, these results indicate a transition from Caspase-9- to Bax- and Bcl-X_L-mediated neuronal apoptosis.

Key words: development; programmed cell death; p53; apoptosis; Bax; Caspase-3

A broad spectrum of death stimuli, including developmental signals, cellular stress, and DNA damage, initiate programmed cell death (apoptosis) (Gross et al., 1999; Vaux and Korsmeyer, 1999). The Bcl-2 and Caspase families of proteins serve as important regulators of apoptotic death. Although Bcl-2 family members share domains of structural homology, some Bcl-2 family proteins function as positive regulators of apoptosis, whereas others act as negative regulators (Dragovich et al., 1998; Reed, 1998). Bcl-X_L, an antiapoptotic member of the Bcl-2 family, critically regulates immature neuron survival during nervous system development (Motoyama et al., 1995). The increased death of Bcl-X_L-deficient neurons can be prevented both *in vivo* and *in vitro* by concomitant Bax deficiency, indicating that these two Bcl-2 family members are in critical balance (Shindler et al., 1997). Bcl-X_L-deficient mice die around embryonic day 13 (E13) because of increased hematopoietic cell death, an effect that is not prevented by Bax deficiency (Motoyama et al., 1995; Shindler et al., 1997). In most cell types, Bcl-2 family action is mediated by their effect on caspase activation. Caspases are synthesized as zymogens; once activated by an apoptotic signal, they cleave a host of key cellular substrates, leading to the morphological and biochemical hallmarks of apoptosis (Nicholson and Thornberry, 1997; Wolf et al., 1999; Zhivotovsky et al., 1999). The Caspase family contains at least 14 members (Ahmad et al., 1998; Hu et al., 1998; Vandecraen et al., 1998), of which Caspases-3 and -9 appear to play particularly significant roles in the developing nervous system.

Targeted gene disruptions of *caspase-9* or *caspase-3* lead to decreased neuronal apoptosis and neurodevelopmental abnormalities including: an expanded ventricular zone, ectopic and duplicated neuronal structures, and gross brain malformations (Kuida et al., 1996, 1998; Hakem et al., 1998). Bcl-X_L-deficient embryos exhibit marked neuronal Caspase-3 activation, and both Bax- and Caspase-9-deficient mice show defective Caspase-3 activation, suggesting a linear activation cascade involving Bcl-X_L, Bax, Caspase-9, and Caspase-3 (Kuida et al., 1998; Hakem et al., 1998; Roth et al., 2000). We recently demonstrated that Caspase-3 deficiency, similar to Bax deficiency, abrogates the increased neuronal apoptosis caused by Bcl-X_L deficiency both *in*

Received Aug. 2, 2000; revised Oct. 9, 2000; accepted Oct. 13, 2000.

This work was supported by grants from the Public Health Service to P.R. and K.A.R. A.U.Z. received fellowship support from the McDonnell Center for Cellular and Molecular Neurobiology. We thank Drs. Jeffrey R. Leonard (Washington University) and C.-Y. Kuan (Yale University) for helpful discussions and review of this manuscript, C. Latham, J. McDonough, and B. Klocke for expert technical assistance, and A. Schmeckebier for secretarial support. CM1 antiserum was generously provided by Dr. A. Srinivasan (IDUN Pharmaceuticals). R.A.F. is an investigator of the Howard Hughes Medical Institute.

Correspondence should be addressed to Dr. Kevin A. Roth, Department of Pathology, Washington University School of Medicine, 660 South Euclid Avenue, Box 8118, St. Louis, MO 63110. E-mail: kroth@pathology.wustl.edu.

vivo and *in vitro,* although it did not prevent increased hematopoietic cell apoptosis or embryonic lethality in Bcl-X_L-deficient mice (Roth et al., 2000).

Whereas the intracellular balance between proapoptotic and antiapoptotic molecules is thought to regulate cell death, it remains unclear whether the antiapoptotic function of Bcl-X_L is necessarily mediated through inhibition of the proapoptotic effects of Caspase-9. To test this possibility, mice carrying disruptions of *bcl-x* and *caspase-9* were interbred, and neuronal apoptosis was examined in *bcl-x*$^{-/-}$/*caspase-9*$^{-/-}$ embryos using both *in vivo* and *in vitro* techniques. Finally, we used primary telencephalic neuron cultures from wild-type embryos and mice with targeted gene disruptions of *bcl-x*, *bax*, *caspase-9*, *caspase-3*, and *p53* to determine which of these molecules are critically involved in DNA damage-induced neuron death.

MATERIALS AND METHODS

Generation of bcl-x/caspase-9 mutant mice. The use of homologous recombination in embryonic stem (ES) cells to generate *bcl-x*$^{-/-}$ (Motoyama et al., 1995) and *caspase-9*$^{-/-}$ (Kuida et al., 1998) mice has been described previously. To generate mice deficient in both Bcl-X_L and Caspase-9, double heterozygote (*bcl-x*$^{+/-}$/*caspase-9*$^{+/-}$) mice were interbred to produce embryos of nine possible genotypes, including *bcl-x*$^{-/-}$/*caspase-9*$^{-/-}$ embryos. Endogenous and disrupted genes were detected by PCR analysis of tail DNA extracts as described previously (Motoyama et al., 1995; Kuida et al., 1998). The morning on which a vaginal plug was detected was assigned E0.5. To determine whether the distribution of generated genotypes followed the predicted Mendelian distribution, χ^2 analysis of contingency tables was used.

Histological preparation of tissue and immunohistochemistry. Pregnant mice were anesthetized with methoxyflurane and killed on gestational day 12.5 by cervical dislocation. Embryos (E12.5) were removed, and tail and limb samples were taken for DNA extractions and PCR analyses. Whole embryos or embryos without their forebrains, which were used for telencephalic cell cultures, were placed in Bouin's fixative overnight at 4°C followed by three washes in 70% ethanol. Tissue was dehydrated, paraffin-embedded, and 4-μm-thick sagittal sections were cut. Sections were deparaffinized and hematoxylin and eosin (H & E)-stained as described previously (Shindler et al., 1997). Alternatively for semithin sections, 2% (v/v) glutaraldehyde-fixed embryos were embedded in plastic, and 1-μm-thick sections were cut and stained with 1% toluidine blue.

For immunohistochemistry, deparaffinized sections were incubated overnight at 4°C with CM-1, an affinity-purified rabbit polyclonal antiserum, which recognizes the p18 subunit of activated Caspase 3 (Srinivasan et al., 1998), diluted 1:40,000 in PBS-blocking buffer (PBS-BB: PBS with 0.1% BSA, 0.3% Triton X-100, and 0.2% nonfat powdered dry milk). After washes with PBS, sections were incubated with a donkey anti-rabbit horseradish peroxidase-conjugated secondary antibody (Jackson ImmunoResearch, West Grove, PA), diluted 1:1000 in PBS-BB, for 1 hr at room temperature. Immunostaining was detected using a tyramide signal amplification system (NEN Life Science Products, Boston, MA). Tissue was counterstained with bisbenzimide (0.2 μg/ml; Hoechst 33258; Sigma, St. Louis, MO) and examined with a Zeiss-Axioskop microscope equipped with epifluorescence.

Terminal deoxynucleotidyl transferase-mediated biotinylated UTP nick end labeling staining. Terminal deoxynucleotidyl transferase-mediated biotinylated UTP nick end labeling (TUNEL) reactions were done with slight modifications of a method described previously (Tornusciolo et al., 1995). Briefly, tissue sections were deparaffinized and permeabilized with 0.5% Triton X-100 in PBS (0.1 M PBS, pH 7.4) for 10 min at room temperature. Sections were subsequently incubated with terminal deoxynucleotidyl transferase (TDT; 3.125 U/100 l of buffer; Roche Molecular Biochemicals, Indianapolis, IN) and digoxigenin-conjugated deoxyuridine triphosphate (0.125 nmol/100 l of buffer; Roche Molecular Biochemicals) for 60 min at 37°C in TDT buffer (30 mM Tris-base, pH 7.2, 140 mM sodium cacodylate, and 1 mM cobalt chloride). Reactions were stopped by incubating tissues for 15 min in a solution of 300 mM sodium chloride and 30 mM sodium citrate. TDT-reacted tissues were incubated overnight at 4°C with horseradish peroxidase-conjugated sheep anti-digoxigenin antiserum (Roche Molecular Biochemicals) diluted 1:1000 in PBS-blocking buffer. After washes with PBS, labeled cells were visualized by tyramide signal amplification with cyanine-3 tyramide (NEN Life Science Products). Tissue was counterstained with bisbenzimide (Hoechst 33258; Sigma) and visualized on a Zeiss-Axioskop microscope equipped with epifluorescence. Apoptosis in E12.5 dorsal root ganglia (DRG) and liver was assessed by counting TUNEL-positive cells in multiple 60× fields for each embryo analyzed.

Primary telencephalic cultures. E12.5 telencephalic cells were dissociated as described previously (Flaris et al., 1995; Shindler and Roth, 1996). Briefly, embryos were removed on gestational day 12.5. Telencephalic vesicles were isolated, and cells were dissociated for 15 min at 37°C in HBSS (Life Technologies, Grand Island, NY) containing 0.01% trypsin with 0.004% EDTA, 0.02 mg/ml DNase I, and 0.1% BSA (all purchased from Sigma). Trypsinization was stopped by adding an equal volume of DMEM containing 10% fetal calf serum (FCS) followed by mild trituration with a fire-polished Pasteur pipette. Dissociated cells from each embryo were washed once with HBSS followed by HBSS with 0.2% BSA. A small sample from each embryo was stained with Trypan blue and counted. A total of 20,000 cells, diluted in DMEM, were plated per well of a 48 well tissue culture plate that was precoated with successive overnight incubations in 0.1 mg/ml poly-L-lysine (Sigma) and 0.01 mg/ml laminin (Collaborative Biomedical Products, Bedford, MA). Cultures were incubated for 48 hr at 37°C in humidified 5% CO_2 and 95% air atmosphere in DMEM. Propidium iodide (PI; 0.5 μg/ml; Molecular Probes, Eugene, OR) was added 15 min before fixation to label dead cells. Cultures were then fixed with Bouin's fixative for 20 min at 4°C. Fixed cells were incubated at 4°C overnight with CM-1, diluted 1:100,000 in PBS-BB (without Triton X-100), and washed several times with PBS. Bound antibody was detected using donkey anti-rabbit horseradish-peroxidase and tyramide signal amplification with fluorescein–tyramide (NEN Life Sciences). Cells were counterstained with bisbenzimide and visualized. The number of nuclei (bisbenzimide-stained), CM1-immunoreactive cells, and PI-positive nuclei were counted at 40× magnification from multiple randomly selected fields. Approximately 150–200 nuclei were counted per well, and all conditions were performed in duplicate for each embryo. Significance was established using the Mann–Whitney rank sum test.

AraC treatment of matured telencephalic neuron cultures. The use of homologous recombination in ES cells to generate *bcl-x*$^{-/-}$ (Motoyama et al., 1995), *bax*$^{-/-}$ (Shindler et al., 1997), *caspase-9*$^{-/-}$ (Kuida et al., 1998), and *caspase-3*$^{-/-}$ (Kuida et al., 1996) mice have been described previously. *p53*$^{+/-}$ and *p53*$^{-/-}$ mice were purchased from Taconic (Germantown, NY). Heterozygous mice were interbred to generate wild-type, heterozygous, and homozygous mutant mice. Endogenous and disrupted genes were detected by PCR analysis of tail DNA extracts (Timme and Thompson, 1994; Motoyama et al., 1995; Kuida et al., 1996; Shindler et al., 1997; Kuida et al., 1998). Cells were plated in ITS, a chemically defined serum-free medium containing insulin, transferrin, selenium, progesterone, putrescine, glucose, and glutamine (Roth et al., 1996) and incubated at 37°C in humidified 5% CO_2 and 95% air atmosphere for 48 hr. Cells were then placed in fresh medium containing 2% FCS with or without 100 μM AraC (Sigma) for an additional 48 hr. SYTOX green (500 nM; SG; Molecular Probes) was added to label dead cells. Cultures were fixed with 4% paraformaldehyde, pH 7.4, for 20 min at 4°C and stained with CM1 antiserum as described above. Immunostaining was detected using donkey anti-rabbit horseradish-peroxidase, diluted 1:1000, and visualized by tyramide signal amplification with cyanine 3-tyramide (NEN Life Sciences). Cells were counterstained with bisbenzimide (Sigma) and visualized on a Zeiss-Axiovert microscope equipped with epifluorescence. Telencephalic cells from each embryo were plated in duplicate wells for each condition, and the number of nuclei, CM1-, and SG-positive cells were counted at 40× magnification from multiple fields in each well. Approximately 150–200 nuclei were counted per well, and significance was established using the Mann–Whitney rank sum test.

DEVD caspase cleavage assay. Telencephalic neurons at 100,000 cells per well were cultured for 48 hr on poly-L-lysine–laminin-coated 48 well plates and treated with 100 μM AraC in the presence or absence of 50 μM BOC-Asp(Ome)-fluoromethylketone (BAF; Enzyme Systems Products, Livermore, CA). Cells were assayed for Caspase-3-like enzymatic activity 12 hr after treatment, using a previously described protocol (Armstrong et al., 1997). Briefly, cells were washed once with PBS and lysed in 100 μl of buffer A (in mM: 10 HEPES, pH 7.4, 42 KCl, 5 $MgCl_2$, 1 DTT, 0.5% 3-([3-cholamidopropyl]dimethylammonio)-1-propane-sulfonate (CHAPS), and 1 PMSF with 1 μg/ml leupeptin). Cells that had been treated with BAF were washed four times with PBS before lysis. Ac-DEVD-7-amino-4-methylcoumarin (AMC) (Biomol, Plymouth Meeting,

Table 1. Genotypes of embryos and live-born mice generated from interbreeding of *bcl-x*$^{+/-}$/*caspase-9*$^{+/-}$ mice

Genotypes (expected frequency, %)	Number of E12.5 mice (%)	Number of live-born mice (%)
bcl-x$^{+/+}$/*casp9*$^{+/+}$ (6.25)	6 (4.3)	22 (31.9)
bcl-x$^{+/+}$/*casp9*$^{+/-}$ (12.5)	21 (14.8)	22 (31.9)
bcl-x$^{+/+}$/*casp9*$^{-/-}$ (6.25)	10 (7.1)	3 (4.3)
bcl-x$^{+/-}$/*casp9*$^{+/+}$ (12.5)	14 (9.9)	9 (13.0)
bcl-x$^{+/-}$/*casp9*$^{+/-}$ (25.0)	31 (22.0)	25 (36.2)
bcl-x$^{+/-}$/*casp9*$^{-/-}$ (12.5)	24 (17.0)	0 (0)
bcl-x$^{-/-}$/*casp9*$^{+/+}$ (6.25)	20 (14.2)	0 (0)
bcl-x$^{-/-}$/*casp9*$^{+/-}$ (12.5)	9 (6.4)	0 (0)
bcl-x$^{-/-}$/*casp9*$^{-/-}$ (6.25)	6 (4.3)	0 (0)

Nine different genotypic combinations resulted from the interbreeding of *bcl-x*$^{+/-}$/*caspase-9*$^{+/-}$ mice, shown in column 1. A total of 141 E12.5 embryos were generated in 23 litters. All nine genotypes were found and followed the predicted Mendelian distribution. Sixty-nine live-born mice were generated in 15 litters. No *bcl-x*$^{-/-}$ were born, indicating that these mice were embryonic lethal. Live-born *caspase-9*$^{-/-}$ mice were also rare, consistent with perinatal lethality.

PA) at a final concentration of 10 μM in 200 μl of buffer B (25 mM HEPES, pH 7.4, 1 mM EDTA, 0.1% CHAPS, 10% sucrose, and 3 mM DTT) was added and incubated for 20 min at room temperature in the dark. The generation of the fluorescent amc cleavage product was measured at excitation 360 nm, emission 460 nm, every 2 min for 2 hr, using a Bio-Tek Instruments (Winooski, VT) FL_X800 fluorescent plate reader. Ac-DEVD-AMC cleavage activity was expressed relative to untreated controls.

RESULTS

Caspase-9 deficiency does not prevent embryonic lethality in Bcl-X_L-deficient mice

To determine whether Caspase-9 deficiency is capable of rescuing embryonic lethality in *bcl-x*$^{-/-}$ mice, *bcl-x*$^{+/-}$/*caspase-9*$^{+/-}$ mice were interbred. Embryos harvested at E12.5, before the lethal effect of Bcl-X_L deficiency, followed expected Mendelian frequencies ($p \leq 0.05$). However, genotypic analyses of 15 litters containing 69 live-born pups revealed no *bcl-x*$^{-/-}$/*caspase-9*$^{-/-}$ mice, indicating that mice deficient in both genes are not viable. No live-born *bcl-x*$^{-/-}$ mice and only rare *caspase-9*$^{-/-}$ were found, consistent with our previous reports of *bcl-x*$^{-/-}$ lethality at ~E13 (Motoyama et al., 1995) and extensive perinatal lethality of *caspase-9*$^{-/-}$ mice (Hakem et al., 1998; Kuida et al., 1998) (Table 1).

Caspase-9 deficiency prevents increased apoptosis in the Bcl-X_L-deficient nervous system

The nervous systems of E12.5 wild-type mice exhibited only rare condensed, pyknotic nuclei in the brainstem and spinal cord, when visualized by H & E staining (Fig. 1*A*). As previously demonstrated (Motoyama et al., 1995; Kuida et al., 1998), the nervous systems of E12.5 Bcl-X_L-deficient mice showed increased numbers of apoptotic neurons (Fig. 1*B*), and few apoptotic neurons were observed in *caspase-9*$^{-/-}$ embryos (data not shown). Increased neuronal apoptosis was observed in Bcl-X_L-deficient mice containing either one (*bcl-x*$^{-/-}$/*caspase-9*$^{+/-}$) or two (*bcl-x*$^{-/-}$/*caspase-9*$^{+/+}$) copies of endogenous *caspase-9*. In contrast, neuronal apoptosis in *bcl-x*$^{-/-}$/*caspase-9*$^{-/-}$ mice was reduced to less than that observed in wild-type littermates (Fig. 1*C*). This indicates that Caspase-9 deficiency blocks the increased apoptosis of Bcl-X_L-deficient immature neurons.

As shown previously, *in situ* detection revealed a dramatic increase in the number of activated Caspase-3-immunoreactive cells in the Bcl-X_L-deficient nervous system (Srinivasan et al., 1998) (Fig. 1*D,E*) and few if any immunoreactive cells in Caspase-9-deficient E12.5 embryos (data not shown). Caspase-9 deficiency completely prevented the increased Caspase-3 activation and neuronal apoptosis observed in Bcl-X_L-deficient embryos (Fig. 1*F*).

Bcl-X_L-deficiency does not prevent neurodevelopmental pathology in *caspase-9*$^{-/-}$ mice

Bcl-x$^{-/-}$/*caspase-9*$^{-/-}$ embryos were examined to determine whether Bcl-X_L deficiency could prevent the Caspase-9-deficient neuronal phenotype. Similar to Caspase-9-deficient mice, Bcl-X_L-/Caspase-9 double-deficient mice were grossly abnormal (6 of 6 *bcl-x*$^{-/-}$/*caspase-9*$^{-/-}$ embryos) and exhibited neurodevelopmental pathology, including exencephaly, expanded ventricular zones, and cortical dysplasia, indicating that Bcl-X_L deficiency is incapable of rescuing the *caspase-9*$^{-/-}$ neuronal phenotype (Fig. 2*A–C*).

Quantification of apoptosis in E12.5 DRG and liver

Quantitative analysis of TUNEL-positive cells in E12.5 mice demonstrated that the number of apoptotic cells in *bcl-x*$^{-/-}$ DRG was more than twice that observed in wild-type DRG (Table 2). Apoptosis was reduced by 89% in *caspase 9*$^{-/-}$ DRG compared with wild-type DRG. The increased apoptosis observed in the *bcl-x*$^{-/-}$ DRG was suppressed in *bcl-x*$^{-/-}$/*caspase-9*$^{-/-}$ embryos

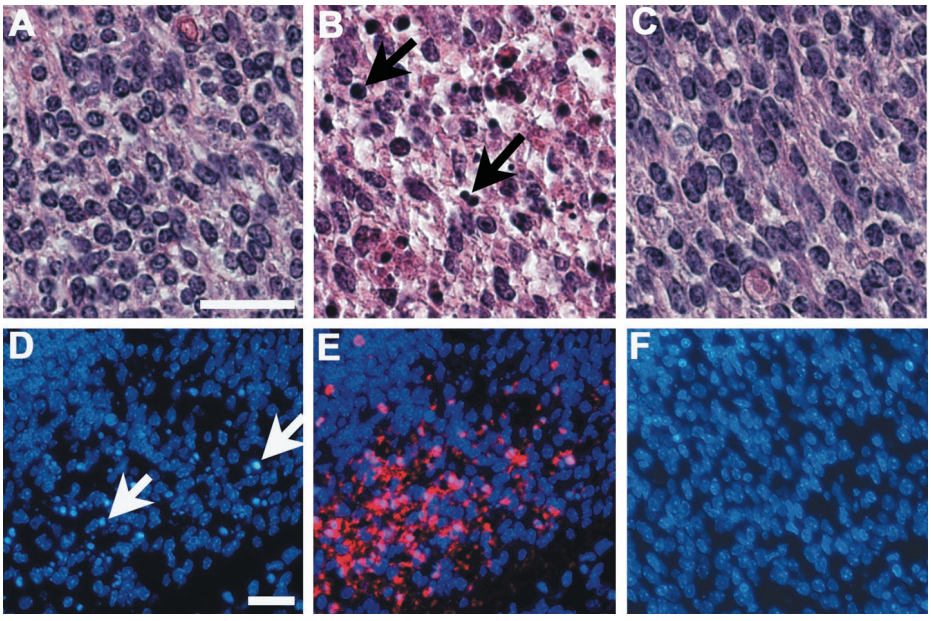

Figure 1. Caspase-9 deficiency blocks the increased immature neuron apoptosis caused by Bcl-X_L deficiency. *A–C,* Hematoxylin and eosin-stained sections from the E12.5 brainstem show normal healthy neurons in a wild-type embryo (*A*) and large numbers of apoptotic neurons in a Bcl-X_L-deficient embryo (*B*; examples of apoptotic nuclei are indicated by *arrows*). *Bcl-x*$^{-/-}$/*caspase-9*$^{-/-}$ brainstem (*C*) shows no evidence of increased apoptosis. *D–F,* A bisbenzimide-stained section from a Bcl-X_L-deficient embryo shows frequent abnormal condensed nuclei in the anterior spinal cord (*D*; examples indicated by *arrows*), and simultaneous labeling for activated Caspase-3 immunoreactivity (*E, red*) reveals numerous positive cells. Dual staining for activated Caspase-3 immunoreactivity and nuclei in a *bcl-x*$^{-/-}$/*caspase-9*$^{-/-}$ E12.5 spinal cord (*F*) shows neither activated Caspase-3 immunoreactivity nor condensed nuclei. Scale bar, 25 μm.

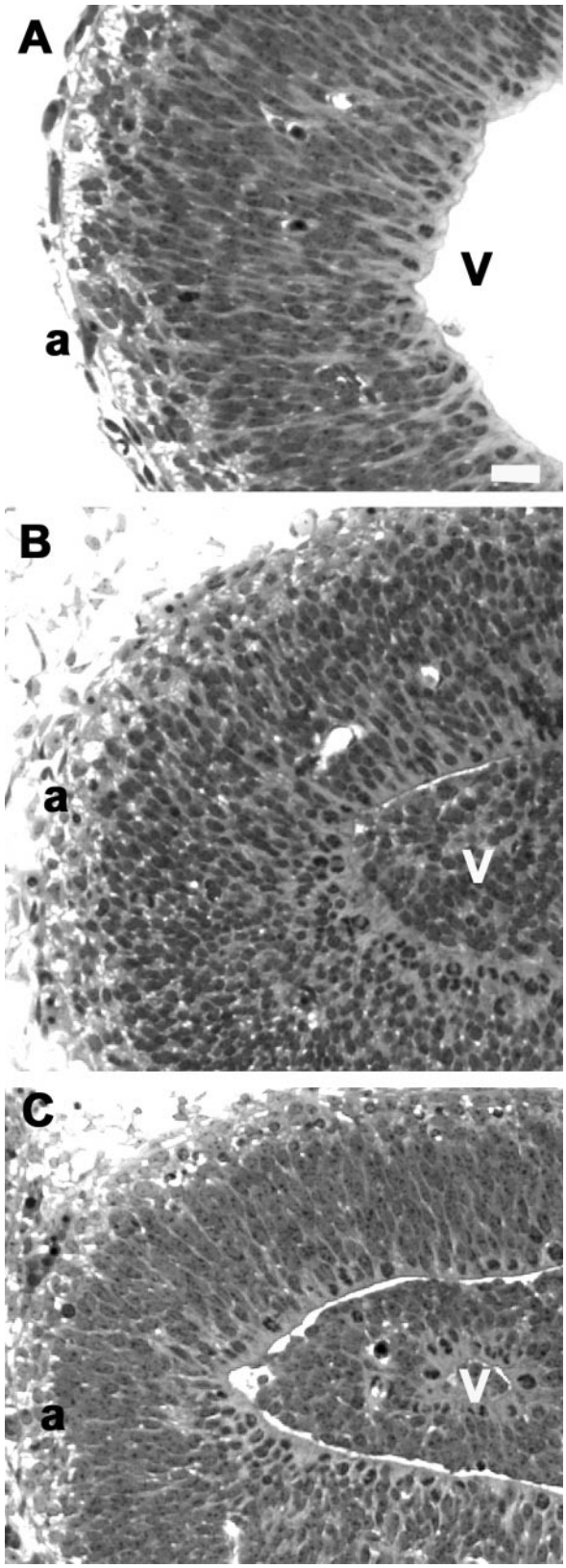

Figure 2. Bcl-X_L deficiency fails to prevent neurodevelopmental abnormalities in Caspase-9-deficient embryos. Toluidine blue-stained horizontal sections from the E12.5 telencephalon show well organized neuroepithelium in wild-type (*A*) but neither *caspase-9*$^{-/-}$ (*B*) nor *bcl-x*$^{-/-}$/*caspase-9*$^{-/-}$ (*C*) embryos. In both Caspase-9-deficient embryos, the telencephalic vesicle is thickened, and supernumerary cells fill the lateral ventricle (*V*). *a,* Anterior. Scale bar, 25 μm.

Table 2. Apoptosis in E12.5 dorsal root ganglia and liver

Genotype (*n*)	Dorsal root ganglia (cells/field)	Liver (cells/field)
bcl-x$^{+/*}$/*casp9*$^{+/*}$ (6)	7.5 ± 1.1	9.9 ± 1.5
bcl-x$^{-/-}$/*casp9*$^{+/*}$ (6)	17.2 ± 1.4*	21.0 ± 1.2*
bcl-x$^{+/*}$/*casp9*$^{-/*}$ (7)	0.8 ± 0.4*	10.6 ± 1.8
bcl-x$^{-/*}$/*casp9*$^{-/*}$ (4)	0.7 ± 0.8*	18.2 ± 1.4*

Bouin's fixed sagittal sections from paraffin-embedded E12.5 *bcl-x*$^{+/*}$/*casp9*$^{+/*}$, *bcl-x*$^{-/-}$/*casp9*$^{+/*}$, *bcl-x*$^{+/*}$/*casp9*$^{-/-}$, and *bcl-x*$^{-/-}$/*casp9*$^{-/-}$ mice were TUNEL-labeled (* denotes + or −). The number of embryos analyzed is shown in parentheses. The mean number of positive cells and SEM per 60× field were determined for each group.

*$p < 0.05$ versus bcl-x $^{+/*}$/casp9 $^{+/*}$ using Kruskal–Wallis ANOVA on ranks.

to levels significantly lower than that detected in wild-type DRG. At E12.5, the embryonic liver consists of a mixed population of hepatic and hematopoietic cells. Bcl-X_L deficiency causes embryonic lethality secondary to its effects on hematopoietic cells, particularly erythroid elements. *Bcl-x*$^{-/-}$ livers demonstrated a twofold increase in the number of TUNEL-positive cells compared with wild-type livers. Caspase-9 deficiency alone had no effect on the number of TUNEL-positive cells detected in the liver. In *bcl-x*$^{-/-}$/*caspase-9*$^{-/-}$ livers, the number of apoptotic cells was similar to that observed in Bcl-X_L-deficient livers, indicating that Caspase-9 deficiency did not suppress the increased hematopoietic cell apoptosis in *bcl-x*$^{-/-}$ mice.

Caspase-9 deficiency prevents increased apoptosis of Bcl-X_L-deficient telencephalic cells *in vitro*

Short-term (0–48 hr) primary telencephalic cell cultures were used to further examine the interaction between Bcl-X_L and Caspase-9 in immature neurons. Initially, these cultures consist predominantly of neural precursor cells; ~70% nestin and 25% MAP2-immunoreactive cells, the majority of which have yet to extend neurites. Over the 48 hr culture period, the vast majority of cells exit the cell cycle and develop MAP2-immunoreactive processes (D'Sa-Eipper and Roth, 2000). We previously demonstrated that Bcl-X_L-deficient telencephalic cells show similar levels of apoptosis as wild-type cultures at time 0 but show increased apoptosis at 48 hr if grown in minimal medium (Roth et al., 1996). This *in vitro* effect is analogous to the increased immature neuron apoptosis observed in Bcl-X_L-deficient embryos *in vivo*. As expected after 48 hr in DMEM, Bcl-X_L-deficient telencephalic neurons had significantly greater Caspase-3 activation and cell death compared with wild-type neurons (Fig. 3). *Bcl-x*$^{-/-}$/*caspase-9*$^{-/-}$ mice exhibited significantly reduced cell death compared with *bcl-x*$^{-/-}$/*caspase-9*$^{+/+}$ and *bcl-x*$^{-/-}$/*caspase-9*$^{+/-}$ littermates. Caspase-3 activation was virtually absent in all Caspase-9-deficient mice (Fig. 3). These *in vitro* results support the *in vivo* finding that Caspase-9 deficiency rescues Bcl-X_L-deficient immature neurons from excess apoptotic death. Caspase-9 deficiency alone produced a slight but statistically insignificant decrease in baseline cell death (Fig. 3). The baseline cell death in our telencephalic cell cultures appeared to be both Caspase-3- and Caspase-9-independent and may reflect necrotic cell death secondary to suboptimal trophic factor support under these serum-free conditions.

p53-deficient and Bax-deficient, but not Caspase-9-deficient or Caspase-3-deficient, telencephalic neurons are protected against AraC-induced death

Unlike telencephalic cells grown for 48 hr in minimal medium, Bcl-X_L-deficient and wild-type telencephalic neurons maintained

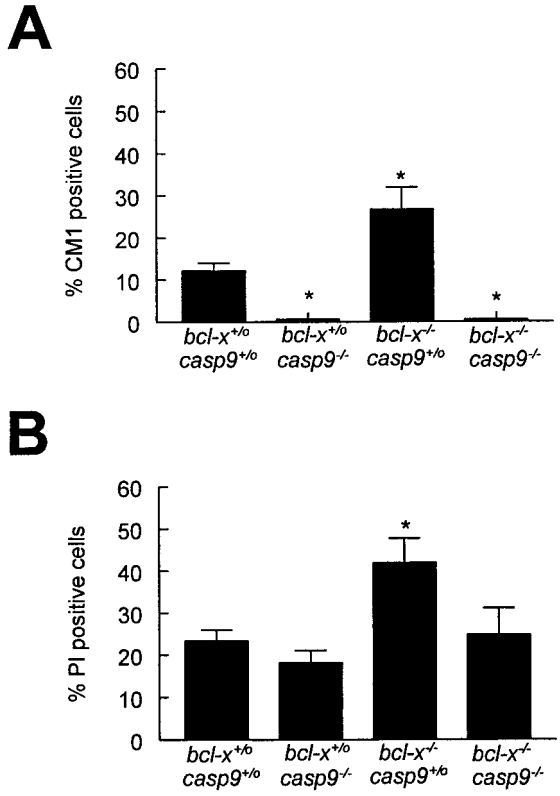

Figure 3. Quantification of Caspase-3 activation and cell death in wild-type, Caspase-9-deficient, Bcl-X_L-deficient, and double-deficient telencephalic cells. E12.5 telencephalic cells were grown for 48 hr in DMEM; activated Caspase-3 immunoreactive cells were detected with CM1 antiserum (*A*), and cell death (*B*) was determined by propidium iodide labeling. Bcl-X_L-deficient cells had increased Caspase-3 activation and cell death; concomitant Caspase-9 deficiency inhibited the death-promoting effects of Bcl-X_L in this *in vitro* paradigm. No effect of gene dosage on Caspase-3 activation or cell viability was observed for either *bcl-x* or *caspase-9*, and therefore, data from wild-type and heterozygous mutants were pooled (+/o denotes +/+ and +/− mice). Each data point represents the mean ± SEM. $^*p < 0.05$ compared with *bcl-x* $^{+/o}$/*caspase-9* $^{+/o}$ cells.

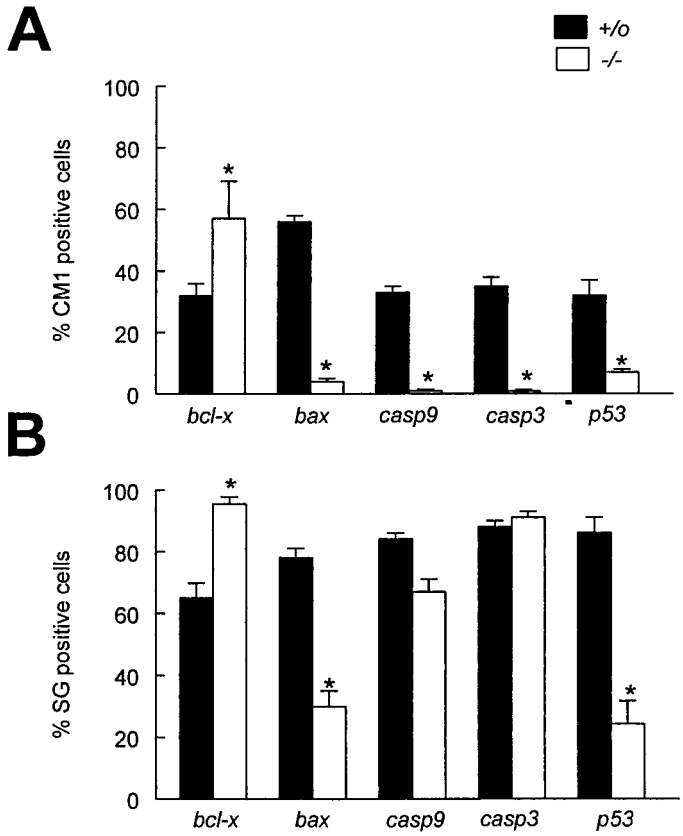

Figure 4. Effect of proapoptotic and antiapoptotic gene disruptions on AraC-induced telencephalic neuron Caspase-3 activation and cell death. Primary telencephalic neuron cultures were prepared from control and homozygous mutant embryos. After 48 hr of AraC exposure, Caspase-3 activation and cell death was assessed using CM1 antiserum and SYTOX Green labeling. In Bcl-X_L-deficient neurons, AraC treatment produced a significant increase in the number of cells exhibiting activated Caspase-3 immunoreactivity (*A*) and in dead cells (*B*). Although Bax-, Caspase-9-, Caspase-3-, and p53-deficient neurons all exhibited reduced Caspase-3 activation compared with control neurons after AraC exposure, only Bax- and p53-deficient neurons exhibited significant neuroprotection. Heterozygous *bax*, *caspase-9*, and *caspase-3* mutant neurons behaved identically to wild-type neurons and therefore, data from wild-type and +/− cultures were pooled (+/o denotes +/+ and +/− mice). In contrast, *p53* $^{+/-}$ neurons exhibited an intermediate degree of neuroprotection (data not shown) and therefore, only wild-type littermates were used to compare the effects of p53 deficiency. Each data point represents mean ± SEM (n = 5–20 for the different genotypes).

in an enriched medium for 48 hr show a comparable degree of baseline death (Roth et al., 1996; Shindler et al., 1998); however, Bcl-X_L-deficient neurons are markedly susceptible to subsequent apoptotic insults. To determine whether Caspase-9 critically regulates telencephalic neuron apoptosis, we examined the death-promoting effects of AraC on telencephalic neuron cultures prepared from wild-type, *bcl-x* $^{-/-}$, and *caspase-9* $^{-/-}$ embryos. These results were compared with the effects of AraC on neurons derived from mice lacking the proapoptotic molecules p53, Bax, or Caspase-3.

In the absence of AraC, baseline neuron viability was ~90%, and there was no significant difference between homozygous gene-disrupted mice and their littermate controls (data not shown). Only rare wild-type cells (~3%) exhibited activated Caspase-3 immunoreactivity at baseline, and few if any activated Caspase-3-immunoreactive cells were detected in untreated *caspase-9* $^{-/-}$, *caspase-3* $^{-/-}$, or *bax* $^{-/-}$ cultures (data not shown). AraC treatment of wild-type telencephalic neuron cultures produced a dramatic concentration-dependent increase in Caspase-3-like enzymatic activity that was completely prevented by the broad caspase inhibitor BAF (DEVD cleavage activity: untreated, 100 ± 6%, n = 5; 100 μM AraC, 414 ± 18%, $^*n$ = 5; AraC + 50 μM BAF, 14 ± 1%, $^*n$ = 5; $^*p < 0.05$ vs untreated cell culture using the Tukey test; additional data not shown). In wild-type cells, AraC caused a marked increase in the percentage of neurons exhibiting activated Caspase-3 immunoreactivity and in dead cells (Fig. 4). These effects were exacerbated in Bcl-X_L-deficient cells (Fig. 4). Caspase-3-deficient neurons exhibited no activated Caspase-3 immunoreactivity, as expected from an effective gene disruption; however, Caspase-3 deficiency provided no protection from AraC-induced neuron death (Fig. 4). In contrast, AraC-exposed *bax* $^{-/-}$ neurons showed both decreased Caspase-3 activation and neuron death compared with AraC-treated wild-type cells (Fig. 4). Caspase-9 typically lies between Bax and Caspase-3 in the neuronal apoptotic pathway, and although *caspase-9* $^{-/-}$ neurons showed no activated Caspase-3 immunoreactivity in response to AraC exposure, they exhibited only limited protection against AraC-induced death (Fig. 4). p53

deficiency provided a similar level of neuroprotection as Bax deficiency against AraC-induced Caspase-3 activation and neuron death (Fig. 4). AraC-treated $p53^{+/-}$ neurons exhibited a small but significantly increased viability compared with $p53^{+/+}$ cells (data not shown). In total, these findings suggest that in telencephalic neurons, AraC induces a p53-dependent and a Bax-dependent death that requires neither Caspase-9 nor Caspase-3 activation.

DISCUSSION

The significance of the Bcl-2 and Caspase families in regulating mammalian cell apoptosis has been demonstrated in a variety of apoptotic paradigms. Along with apoptotic protease activating factor-1 (APAF-1), these molecules are thought to act in a linear death pathway analogous to that controlling programmed cell death in *Caenorhabditis elegans*. We have shown that targeted disruption of *bcl-x*$_L$, a *ced-9* homolog, causes markedly increased apoptosis of immature neurons throughout the developing brain (Motoyama et al., 1995; Roth et al., 1996). This increased death can be prevented either by concomitant disruption of the pro-apoptotic Bcl-2 family member *bax* (Shindler et al., 1997) or by disruption of the *ced-3* homologs, *caspase-9* or *caspase-3* (Roth et al., 2000). As in *C. elegans*, the commitment point to death in immature neurons is activation of an effector caspase. Interestingly, this linear death pathway does not regulate hematopoietic cell death or naturally occurring neural precursor cell death.

The inability of Caspase-9 deficiency to rescue hematopoietic cell death and lethality in Bcl-X_L-deficient embryos indicates that not all biological functions of Bcl-X_L require downstream Caspase-9 and/or Caspase-3 activation. Similarly, the non-neuronal effects of Bcl-X_L deficiency are not prevented by concomitant Bax deficiency. Independent of its interaction with Bax, Bcl-X_L may directly facilitate ATP–ADP exchange in mitochondria and form ion channels in biological membranes (Minn et al., 1999; Vander Heiden et al., 1999). At present, we have no evidence of Bax- and/or caspase-independent actions for Bcl-X_L in the nervous system. An alternatively spliced form of *bcl-x*, *bcl-x*$_S$, is proapoptotic and may contribute to the effects of *bcl-x* disruption in some apoptotic paradigms. Bcl-X_S is unlikely to play a significant role in neuronal apoptosis because it is expressed at only low or undetectable levels in the embryonic and adult brain (Boise et al., 1993; González-García et al., 1995).

Caspase-9, Caspase-3, or APAF-1 deficiency result in decreased neural precursor cell programmed cell death and marked ventricular zone expansion, a phenotype that is not observed in Bax-deficient embryos (Kuida et al., 1996; Cecconi et al., 1998; Kuida et al., 1998). Similarly, Bcl-X_L immunoreactivity is not detected in the ventricular zone, and there is no apparent effect of Bcl-X_L deficiency on neural precursor cell apoptosis (Roth et al., 2000). Bcl-X_L deficiency was unable to rescue the ventricular zone abnormalities observed in Caspase-9-deficient mice, again suggesting that naturally occurring neural precursor cell death is independent of both Bcl-X_L and Bax. Because Caspase-9-, APAF-1, and Caspase-3-deficient mice exhibit similar morphogenetic abnormalities (Kuida et al., 1996; Cecconi et al., 1998; Kuida et al., 1998) and Caspase-9 and APAF-1 are required for neural precursor cell Caspase-3 activation, the commitment point for naturally occurring neural precursor cell death is likely Caspase-3 activation.

Apoptotic pathways can be remarkably stimulus-specific, and we have recently defined an apoptotic pathway in neural precursor cells that is activated by DNA damage and requires both *p53* and *caspase-9* but neither *caspase-3* nor *bax* expression (D'Sa-Eipper et al., 2000). The complexity of neuronal death pathways is additionally evidenced by our current analysis of AraC-induced telencephalic neuron apoptosis. Like neural precursor cells, p53-deficient telencephalic neurons showed substantial protection against AraC-induced death. However, Caspase-9-deficient neurons were only mildly protected against AraC-induced death, whereas Bax deficiency, which had a minimal effect on neural precursor cell apoptosis, markedly inhibited AraC-induced neuron death. We have previously shown that the apoptosis-inducing effects of amyloid $\beta(1–40)$ on telencephalic neurons could be inhibited by Bax deficiency but not Caspase-3 deficiency or by broad spectrum caspase inhibition (Selznick et al., 2000). In total, these results indicate that apoptotic pathways undergo maturation-dependent changes and that the death commitment point varies depending on the apoptotic stimulus and the state of neuronal differentiation. The delineation of these maturation-dependent and stimulus-specific apoptotic pathways, in combination with the availability of mice with specific gene disruptions, should permit a more detailed analysis of the role of programmed cell death in normal nervous system development and in neuropathological conditions. For example, recent studies of Bax- and p53-deficient mice have demonstrated roles for both p53- and Bax-dependent, and p53-dependent, Bax-independent neuronal apoptosis in response to ionizing radiation (Chong et al., 2000). In a second study, cerebellar granule cell neurodegeneration in *lurcher* mice was found to be Bax-dependent but p53-independent (Doughty et al., 2000). In both of these reports, Caspase-3 activation was detected, indicating that identical downstream components of an apoptotic pathway can be activated by distinct upstream mechanisms. In total, these studies demonstrate that the significance of Caspase-9 and Caspase-3 activation to neuronal death depends on both the apoptotic stimulus and the differentiation state of the cell.

REFERENCES

Ahmad M, Srinivasula SM, Hegde R, Mukattash R, Fernandes-Alnemri T, Alnemri ES (1998) Identification and characterization of murine caspase-14, a new member of the caspase family. Cancer Res 58:5201–5205.

Armstrong RC, Aja TJ, Hoang KD, Gaur S, Bai X, Alnemri ES, Litwack G, Karanewsky DS, Fritz LC, Tomaselli KJ (1997) Activation of the CED3/ICE-related protease CPP32 in cerebellar granule neurons undergoing apoptosis but not necrosis. J Neurosci 17:553–562.

Boise LH, González-García M, Postema CE, Ding L, Linsten T, Turka LA, Mao X, Thompson CB (1993) *bcl-x*, a *bcl-2*-related gene that functions as a dominant regulator of apoptotic cell death. Cell 74:597–608.

Cecconi F, Alvarez-Bolado G, Meyer BI, Roth KA, Gruss P (1998) Apaf1 (CED-4 Homolog) regulates programmed cell death in mammalian development. Cell 94:727–737.

Chong MJ, Murray MR, Gosink EC, Russell HRC, Srinivasan A, Kapsetaki M, Korsmeyer SJ, McKinnon PJ (2000) Atm and Bax cooperate in ionizing radiation-induced apoptosis in the central nervous system. Proc Natl Acad Sci USA 97:889–894.

D'Sa-Eipper C, Roth KA (2000) Caspase regulation of neuronal precursor cell apoptosis. Dev Neurosci 22:116–124.

D'Sa-Eipper C, Leonard JR, Putcha G, Zheng TS, Flavell RA, Rakic P, Kuida K, Roth KA (2000) DNA damage-induced precursor cell apoptosis requires p53 and caspase-9 but neither Bax nor caspase-3. Development, in press.

Doughty ML, De Jager PL, Korsmeyer SJ, Heintz N (2000) Neurodegeneration in *Lurcher* mice occurs via multiple cell death pathways. J Neurosci 20:3687–3694.

Dragovich T, Rudin CM, Thompson CB (1998) Signal transduction pathways that regulate cell survival and cell death. Oncogene 17:3207–3213.

Flaris NA, Shindler KS, Kotzbauer PT, Chand P, Ludwig CP, Konstantinidou AD, Roth KA (1995) Developmentally-regulated lectin binding in the embryonic mouse telencephalon. Brain Res 678:99–109.

González-García M, Garcia I, Ding L, O'Shea S, Boise LH, Thompson

CB, Nuñez G (1995) *bcl-x* is expressed in embryonic and postnatal neural tissues and functions to prevent neuronal cell death. Proc Natl Acad Sci USA 92:4304–4308.

Gross A, Yin X-M, Wang K, Wei MC, Jockel J, Milliman C, Erdjument-Bromage H, Tempst P, Korsmeyer SJ (1999) Caspase cleaved BID targets mitochondria and is required for cytochrome c release, while BCL-X_L prevents this release but not tumor necrosis factor-R1/Fas death. J Biol Chem 274:1156–1163.

Hakem R, Hakem A, Duncan GS, Henderson JT, Woo M, Soengas MS, Elia A, de la Pompa JL, Kägi D, Shoo W, Potter J, Yoshida R, Kaufman SA, Lowe SW, Penninger JM, Mak TW (1998) Differential requirement for caspase-9 in apoptotic pathways *in vivo*. Cell 94:339–352.

Hu SM, Snipas SJ, Vincenz C, Salvesen G, Dixit VM (1998) Caspase-14 is a novel developmentally regulated protease. J Biol Chem 273:29648–29653.

Kuida K, Zheng TS, Na S, Kuan C-Y, Yang D, Karasuyama H, Rakic P, Flavell RA (1996) Decreased apoptosis in the brain and premature lethality in CPP32-deficient mice. Nature 384:368–372.

Kuida K, Haydar TF, Kuan C-Y, Gu Y, Taya C, Karasuyama H, Su MSS, Rakic P, Flavell RA (1998) Reduced apoptosis and cytochrome c-mediated caspase activation in mice lacking caspase-9. Cell 94:325–337.

Minn AJ, Kettlun CS, Liang H, Kelekar A, Vander Heiden MG, Chang BS, Fesik SW, Fill M, Thompson CB (1999) Bcl-X_L regulates apoptosis by heterodimerization-dependent and -independent mechanisms. EMBO J 18:632–643.

Motoyama N, Wang F, Roth KA, Sawa H, Nakayama K-I, Nakayama K, Negishi I, Senju S, Zhang Q, Fujii S, Loh DY (1995) Massive cell death of immature hematopoietic cells and neurons in Bcl-x-deficient mice. Science 267:1506–1510.

Nicholson DW Thornberry NA (1997) Caspases killer proteases. Trends Biochem Sci 22:299–306.

Reed JC (1998) Bcl-2 family proteins. Oncogene 17:3225–3236.

Roth KA, Motoyama N, Loh DY (1996) Apoptosis of *bcl-x*-deficient telencephalic cells *in vitro*. J Neurosci 16:1753–1758.

Roth KA, Kuan C-Y, Haydar TF, D'Sa-Eipper C, Shindler KS, Zheng TS, Kuida K, Flavell RA, Rakic P (2000) Epistatic and independent apoptotic functions of Caspase-3 and Bcl-X_L in the developing nervous system. Proc Natl Acad Sci USA 97:466–471.

Selznick LA, Zheng TS, Flavell RA, Rakic, P, Roth KA (2000) Amyloid beta-induced death is Bax-dependent but caspase-independent. J Neuropathol Exp Neurol 59:271–279.

Shindler KS, Roth KA (1996) Double immunofluorescent staining using two unconjugated primary antisera raised in the same species. J Histochem Cytochem 44:1331–1335.

Shindler KS, Latham CB, Roth KA (1997) *bax* deficiency prevents the increased cell death of immature neurons in *bcl-x*-deficient mice. J Neurosci 17:3112–3119.

Shindler KS, Yunker AMR, Cahn R, Zha J, Korsmeyer SJ, Roth KA (1998) Trophic support promotes survival of *bcl-x*-deficient telencephalic cells *in vitro*. Cell Death Differ 5:901–910.

Srinivasan A, Roth KA, Sayers RO, Shindler KS, Wong AM, Fritz LC, Tomaselli KJ (1998) *In situ* immunodetection of activated caspase-3 in apoptotic neurons in the developing nervous system. Cell Death Differ 5:1004–1016.

Timme T, Thompson TC (1994) Rapid allelotype analysis of p53 knockout mice. BioTechniques 17:461–463.

Tornusciolo DRZ, Schmidt RE, Roth KA (1995) Simultaneous detection of TDT-mediated dUTP-biotin nick end-labeling (TUNEL)-positive cells and multiple immunohistochemical markers in single tissue sections. BioTechniques 19:2–7.

Vandecraen M, Vanloo G, Pype S, Vancriekinge W, Vandenbrande I, Molemans F, Fiers W, Declercq W, Vandenabeele P (1998) Identification of a new caspase homologue—caspase-14. Cell Death Differ 5:838–846.

Vander Heiden MG, Chandel NS, Schumacker PT, Thompson CB (1999) Bcl-X_L prevents cell death following growth factor withdrawal by facilitating mitochondrial ATP/ADP exchange. Mol Cell 3:159–167.

Vaux DL, Korsmeyer SJ (1999) Cell death in development. Cell 96:245–254.

Wolf BB, Schuler M, Echeverri F, Green DR (1999) Caspase-3 is the primary activator of apoptotic DNA fragmentation via DNA fragmentation factor-45/inhibitor of caspase-activated DNase inactivation. J Biol Chem 274:30651–30656.

Zhivotovsky B, Samali A, Gahm A, Orrenius S (1999) Caspases: their intracellular localization and translocation during apoptosis. Cell Death Differ 6:644–651.